

## Wear Behaviour of Ferrous Based Thermal Spray Coatings on A356

Ravi Kirpal<sup>a\*</sup>, N.K. Batra<sup>b</sup>, S.Jindal<sup>b</sup>

<sup>a</sup>Department of Mechanical Engineering, TERII, Kurukshetra

<sup>b</sup>Department of Mechanical Engineering, MMU, Mullana

Accepted 10 May 2011, Available online 1 Dec. 2011

### Abstract

Aluminium alloys are becoming a popular choice for engine blocks in automotive industries due to lesser weight as compare to cast iron. Cast A356 Al- alloy, which is a popular choice for automobile engine cylinder block material, has been limited in that use by its poor tribological properties. Many techniques have been explored to solve this problem, including the one addressed in this study, Thermal spray coatings are one of the solutions for improving poor tribological properties of aluminium alloys. In this paper, tribological properties of two types of ferrous based thermal spray coatings were analysed and compared with the cast iron which is a standard material used for cylinder liner. Process used for coating deposition on Al-Si alloy A356 substrate was High Velocity Oxy Fuel (HVOF). The pin and disc tribometer was used to carry out these tests under dry sliding conditions, sliding speed of 1 m/s and 2 m/s, sliding distance of 5000 m and normal load between 9.8 N-73.5 N. Tribological test results showed that, for the investigated conditions coating C-2 had more satisfactory values of wear and friction as compare to C-1 and cast iron, so the former could be adequate substitution for gray cast iron as a material for cylinder blocks.

**Keywords:** High Velocity Oxy Fuel, Ferrous coatings, Microstructure, Sliding wear, Friction.

### 1. Introduction

Engine blocks have traditionally been made of gray cast iron because of the ease of casting (due to absence of appreciable volume shrinkage), machinability, wear resistance, and vibrational damping. Recently, engine manufacturers have been going to aluminum to save weight. Since the mid-1970s, the percentage of aluminum used in automobiles has increased nearly three-fold. The aluminum cast engine blocks now account for more than 60% of automotive engines (Hieuet al, 2005)). The cylinder bore must withstand rapid temperature cycling, repeated shear loading, extreme pressure, and impingement of hot gases, all on the scale of fractions of a second. This demands extremely tight dimensional tolerances and superior wear resistance. For light metal engine blocks, this is traditionally achieved by manufacturing a separate cylinder sleeve, usually made of steel or gray iron. The sleeve can either be press fit into the engine block or suspended in the cylinder block sand mold prior to pouring. Clearly, the melting temperature of the liner material must be well above that of the engine block alloy. The disadvantage of using sleeves in the engine blocks is that the coefficients of thermal expansion of cast iron and aluminum are different. Another approach is to use sleeveless cylinder blocks. However, owing to the softness of aluminum alloys, surface modification is required to enhance the durability so as to

improve their wear and corrosion resistance properties. Thermal spray coating is one of the most versatile methods of depositing coating materials in an effort to enhance the wear and corrosion characteristics ( Kim et al, 2007).

At present, chemical treatments like electroplating of chromium and nickel coatings are becoming increasingly threatened by environmental regulation. Moreover, one should prevent microscopic particles of chromium and nickel, a health hazard, from entering the environment. This process requires complex chemistry and is relatively expensive. Thermal spray coatings are a relatively new solution for cylinder bore protection.

### 2. Thermal spray processes

Advantage of thermal spray process, compared to the other coating processes, is that it has a great range of coating materials, coating thickness and possible coating characteristics.

#### 2.1 Principle of thermal spray process

During the thermal spraying process, melted or molten spray material is propelled, by process gases, onto a cleaned and prepared component surface (Movahedi et al, 2010). The liquid or molten coating particles impact the surface at high speed. This causes the particles to deform into splats and spread like "pancakes" on the substrate. Heat from the hot particles is transferred to the cooler

\* Corresponding author: Ravi Kirpal

base material. As the particles shrink and solidify, they bond to the roughened base material. Adhesion of the coating is therefore based on mechanical “hooking”. Because the adhesion of the coating to the substrate predominantly consists of mechanical bonding, pretreatment of the surface is very important. The surface of the substrate is usually roughened and activated, so the area for bonding of the sprayed particles is increased. The thickness of the sprayed coating is normally between approximately 50  $\mu\text{m}$  and a few mm. The thermal energy used to melt the coating material, may be generally divided into two categories: electrical and flame heating. There are several different processes for thermal spray coating deposition and mostly used are:

- Conventional flame spray
- Electric arc wire spray,
- Plasma spray, and
- High Velocity Oxy-Fuel spray (HVOF).

## 2.2 High Velocity Oxy Fuel Spray

The first HVOF method was introduced in 1982. In the HVOF process the combustion fuel and oxygen are fed to the combustion chamber together with the spray powder (fig.1). The combustion of the gases produces a high temperature and high pressure in the chamber, which causes the supersonic flow of the gases through the nozzle (fig. 2). The powder particles melt because of the flame temperature in the combustion chamber and during the flight through the nozzle. The flame temperature varies in the range of 2500  $^{\circ}\text{C}$  to 3200  $^{\circ}\text{C}$ , depending on the fuel, the fuel gas/oxygen ratio and the gas pressure. In the HVOF process the particles melt completely or only partially, depending on the flame temperature and material’s melting point. The degree of melting depends on the flame temperature and the dwell time in which the particles occupy the flame (Narendra et al, 2001).

These are adjustable process parameters and they affect the properties of the coating. The interest in the HVOF process to produce coatings with a wider range of materials has been growing continuously. For those materials that are sensitive to phase transformations due to evaporation or oxidation, HVOF spray is a very potential coating method due to the process condition, which combines a relatively low flame temperature with a low exposure time in the flame. A few different HVOF spray systems exist with partly different gun designs and capacities. Each one has differences in design, but all are based on the same fundamental principles.

The combination of high pressure (over 4 bar) and gas flow rates of several hundred liters per minute generate hypersonic gas velocities. The system produces an exhaust jet traveling at a speed of about 700 to 2000 m/s.

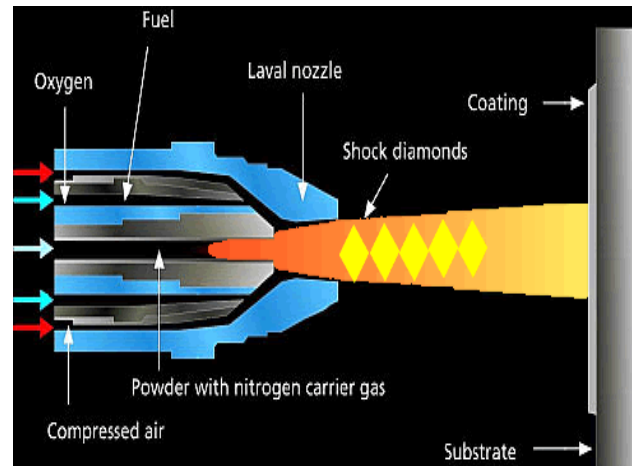


Fig. 1 Schematic diagram of HVOF

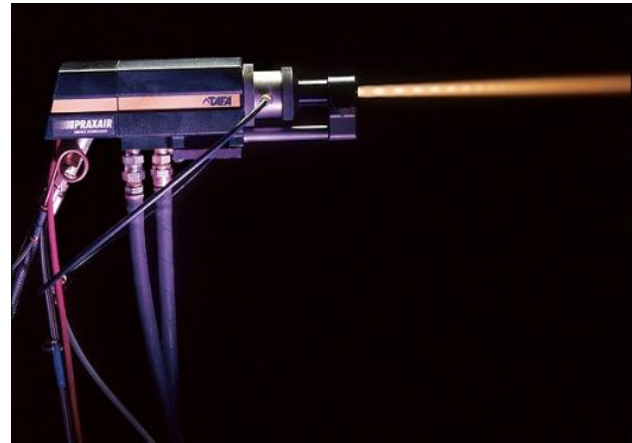


Fig. 2 HVOF gun

Advantages of this spraying technique include good substrate-coating adhesion, high coating density. It is applicable to both metals and ceramics. It involves less set up cost as compared to plasma or detonation gun (Aleksandar et al, 2006).

## 3. Experimental procedure

### 3.1 Materials

Circular discs of diameter 145mm and thickness 3mm were prepared by machining the A356 alloy sheet. For spray material two types of powders were used in this experiment, named C-1 and C-2. The average particle size of both the powders was 50  $\mu\text{m}$ . Gray cast iron (C.I) was chosen as a standard material to compare its performances with the coatings. The discs were casted followed by heating at 500 $^{\circ}\text{C}$  in order to eliminate residual stress in the material and machined to required dimensions. The counter pin was of M42 HSS. The chemical composition of the substrate, counter pin, C.I and spray powders is shown in Tables 1, 2, 3 and 4.

Table 1 Composition of base metal

A356	Element wt %						
	Si	Fe	Cu	Mg	Zn	Ti	Al
	6.72	0.25	0.11	0.27	0.04	0.04	Bal

Table 2 Composition of counter pin

Pin	Element wt %							
	C	Cr	MO	W	V	Co	Mn	Fe
	1.1	3.8	9.5	1.5	1.2	8.0	0.1	Bal

Table 3 Composition of cast iron

Cast Iron	Element wt %					
	C	Si	Mn	P	S	Fe
	3.2	1.5	0.9	0.1	0.1	Bal

Table 4 composition of powders

Powder	Element wt %			
	C	Ni	Cr	Fe
C-1	1.5	9	13	Bal
C-2	2.5	9	13	Bal

### 3.2 Spray conditions

The Praxair TAFA JP-5000® USA system with Praxair 5220 Gun was used in this experiment to deposit the coatings (fig.3). Prior to the spraying process the substrate was firstly degreased and blasted with alumina particles 20-40 µm in size. The coating thickness was measured with Elcometer 456 coating thickness gauges® USA. The HVOF deposition process parameters are shown in table 5.

Table 5 Process parameters

	C-1	C-2
Fuel flow rate	25 l/h	21 l/h
Oxygen flow rate	900 l/min	950 l/min
Torch traverse speed	600 mm/s	600 mm/s
Spray distance	380 mm	380 mm
Powder feed gas	Nitrogen	Nitrogen
Powder size	50 to 60 µm	50 to 60 µm
Compressed air cooling	Yes	Yes
Coating thickness	250±50 µm	250±50 µm

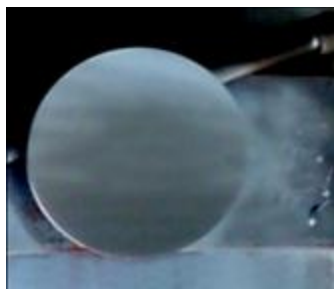


Fig. 3 Coated disc

### 3.3 Microstructure analysis and hardness tests

The coated surface and the microstructure was analysed by Scanning Electron Microscope Zeiss EV040. X-ray diffraction (XRD) studies were carried out using PANalytical X-ray diffractometer (Model X'pert PRO). Ni-filtered CuKα radiation ( $\lambda=1.5148\text{\AA}$ ) was employed with generator setting of 30mA and 40 kV. Continuous scanning was applied with a scanning speed of 10 degrees/min. A range of 2θ from 10 degree to 90 degree was scanned from a fixed slit type, so that all possible diffraction peaks could be detected. The hardness was measured using Vickers hardness tester under a load of 10 kg and microhardness under a load of 300 g using micro Vickers hardness tester. The reported value is an average of 10 measurements.

### 3.4 Tribological testing

#### 3.4 (a) Basic principle of pin and disc tribometer

The pin-on-disc (fig.4) wear test is one of the most spread tests for sliding wear behavior and friction of material pairs. The construction of the test can be both horizontal and vertical, while vertical configuration enables to remove the wear debris during the test. A radius tipped pin is pressed against a flat disc. The relative motion between the two is such that a circumferential wear path on the disc surface is generated. Either the pin or the disc can be moving. The parameters can vary include size and shape of the pin, load, speed and material pairs. The test can be also done in the dry sliding conditions or in the controlled atmosphere and with lubrication (Nicholas et al, 2002).

#### 3.4 (b) Wear tests

Dry sliding wear tests were carried out at room temperature on pin and disc TS 20 Ducom tribometer (fig.5). The disc size was 145 x 3 mm (Diameter x thickness). The wear track diameter was 50 to 100 mm and the counter cylindrical pins were of diameter 6 mm and length 40 mm were used as wear test samples. During all the tests the pin was stationary against the rotating disc. Before and after each test both pin and counter disc were degreased and cleaned of loose debris with acetone. After cleaning both pin and disc were weighed to determine the amount of mass change during the test on an electronic balance having an accuracy of  $\pm 0.001$  g. All the tests were performed as per ASTM G99. Tests were carried out at a constant speed of 1 m/s and 2 m/s, sliding distance of 5000 m and at normal loads of 9.8 N-73.5 N. The wear rate was obtained by dividing the mass loss by total sliding distance (A. Edrisy et al, 2001). The coefficient of friction was automatically monitored with Winducom software. After testing worn surfaces were examined by SEM.

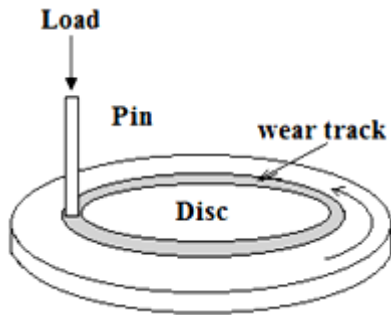


Fig. 4 Basic principle



Fig. 5 Experimental set up

**4. Results and discussion**

*4.1 Coating microstructure and hardness*

By using Praxair TAFA JP-5000® USA system with Praxair 5220 Gun the quality of the coating was good having no sign of cracking. No peeling was seen in the microstructure. Due to the high particle velocities of the HVOF systems, very dense coatings can be produced. In this work, both the coatings had porosity of 1%. Hardness of the coatings and the counter pin is shown in the table 4.

Table 5

Material	Hardness[HV 10]	Microhardness[HV 0.3]
C-1	-	491
C-2	-	524
Pin	243	635
C.I	270	417

X-ray diffraction (XRD) analysis revealed that coating C-1(fig. 5) had elemental iron (Fe), FeNi,  $\alpha$ -Fe<sub>3</sub>O<sub>4</sub>,  $\alpha$ -Fe<sub>2</sub>O<sub>3</sub>, FeO,  $\alpha$ -FeCr, Cr<sub>2</sub>O<sub>3</sub> phases and coating C-2(fig. 6) had elemental iron (Fe),  $\alpha$ -Fe<sub>2</sub>O<sub>3</sub>,  $\gamma$ -Fe<sub>2</sub>O<sub>3</sub>, FeO, Fe<sub>3</sub>Ni,  $\alpha$ -FeCr. Other phases were in small amount, less than 3%

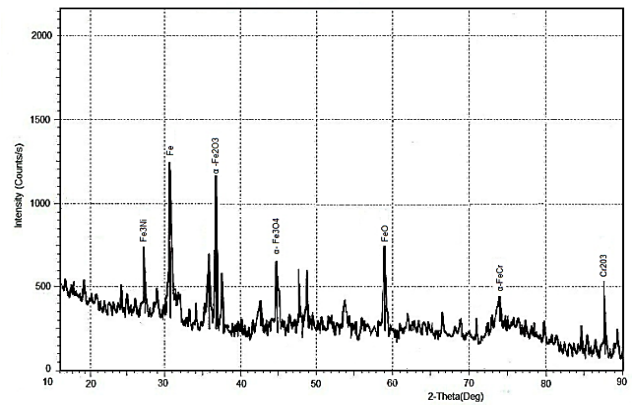


Fig. 6 XRD Spectra of C-1

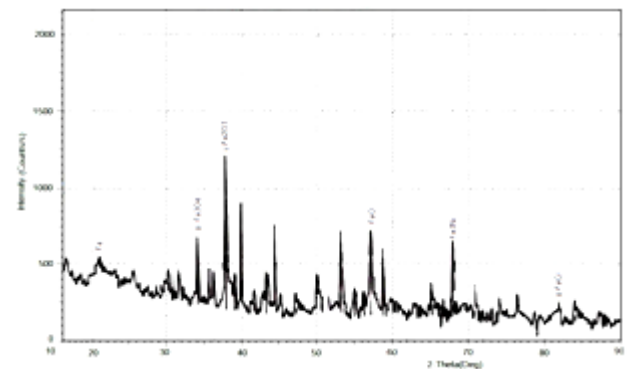


Fig. 7 XRD spectra of C-2

*4.2 Wear rates*

The wear rates were high at low sliding speed but decreased with increasing sliding speed. The effect was found more pronounced at high loads, especially at 49 and 73.5 N in case of coating C-2. At 49N load, for the tests performed at a low sliding speed of 1 m/s, the measured wear rate was 10µg/m; by increasing the sliding speed to 2 m/s the wear rate decreased significantly to 6µg/m. Similarly, at 73.5N load the wear rate decreased from 16µg/m to 10µg/m when the sliding speed increased from 1m/s to 2m/s. However, in coating C-1 at 49N load the wear rate decreased from 12µg/m to 8µg/m by increasing the sliding speed from 1m/s to 2m/s. The effect was not significant at 73.5N load. In case of C.I the higher wear rates as compared to coating C-1 and C-2 were observed. The decrease in wear rates by increasing sliding speed was similar but not significant at the different sliding speeds. The wear rate decreased from 27 to 23µg/m by increasing the speed from 1 to 2 m/s. at 73.5N load. However, it decreased from 6 to 5µg/m at 9.8N load. Variation of wear rate (A. Edrisy et al, 2005) of the coatings and C.I with varying loads and speeds are shown in the fig. 8- 16 along with the coefficient of friction The SEM images of the worn surfaces are shown in fig. 17 (A-H) for coating C-1 at different speeds and loads. Similarly, I-P for coating C-2. The substrate, coating and debris can be seen in the images (K. Bobzin et al, 2008).

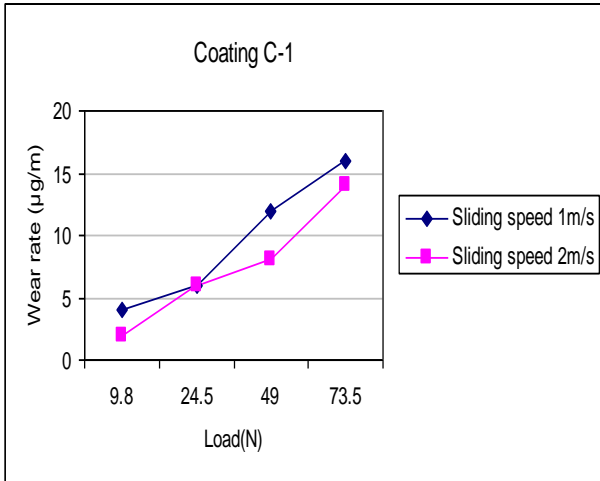


Fig. 8 Wear rates C-1

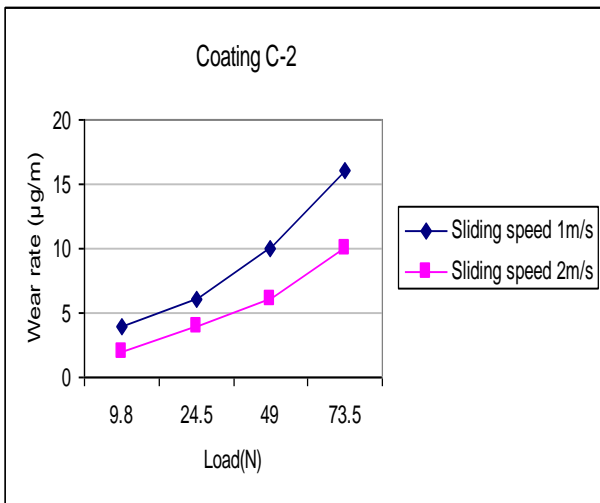


Fig. 9 Wear rates C-2

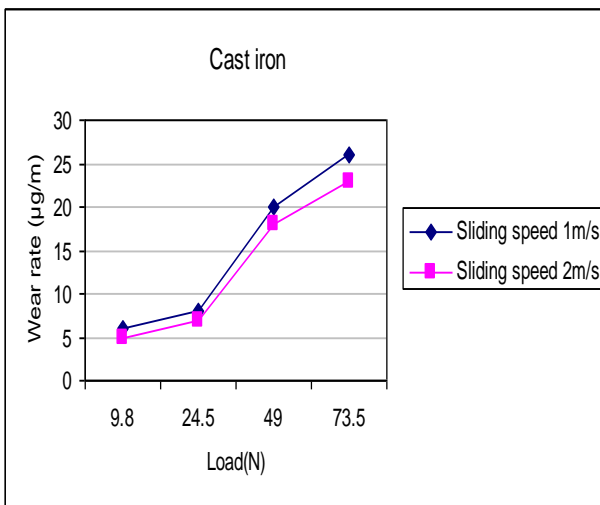


Fig. 10 Wear rates Cast Iron

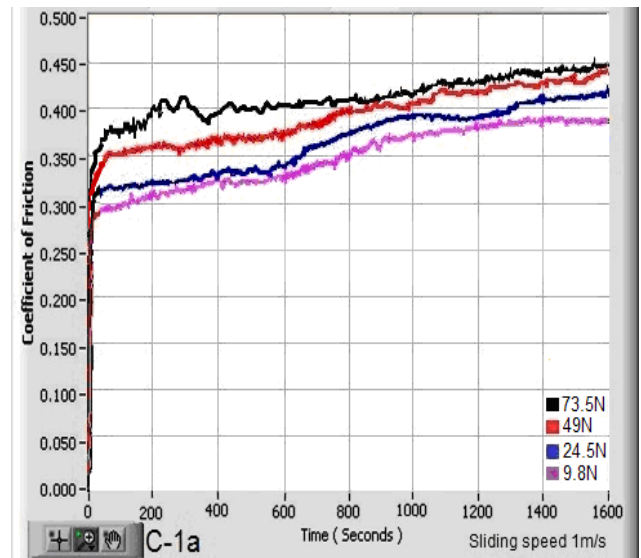


Fig. 11 COF C-1 at 1m/s

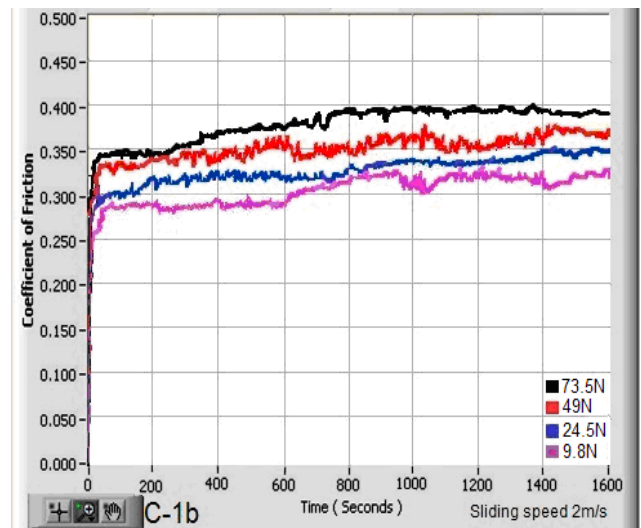


Fig. 12 COF C-1 at 2m/s

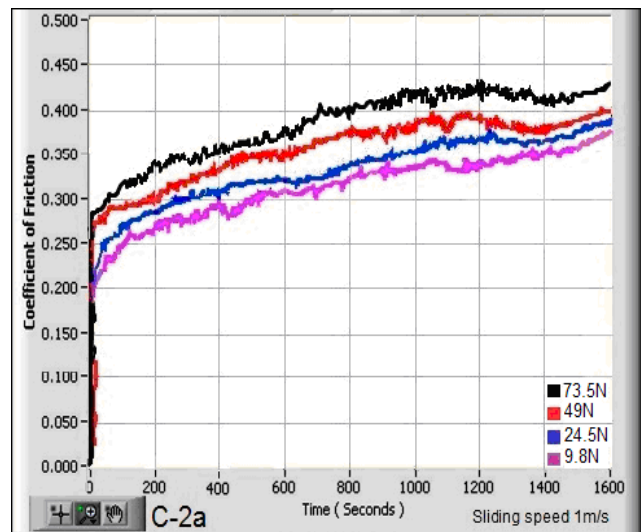


Fig. 13 COF C-2 at 1m/s

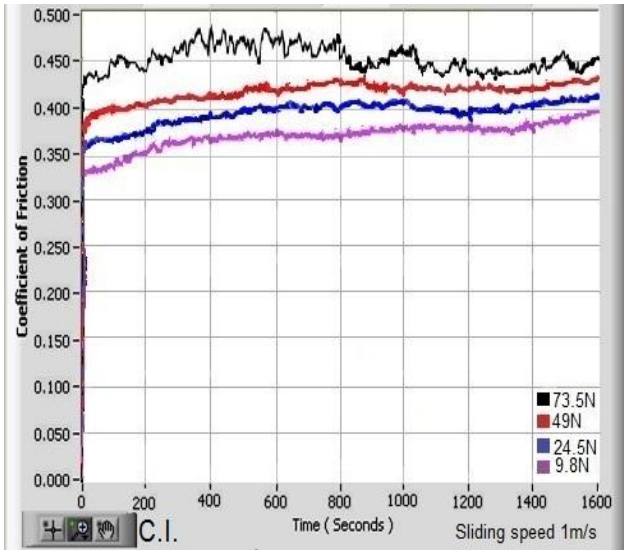


Fig. 14 COF C-2 at 2m/s

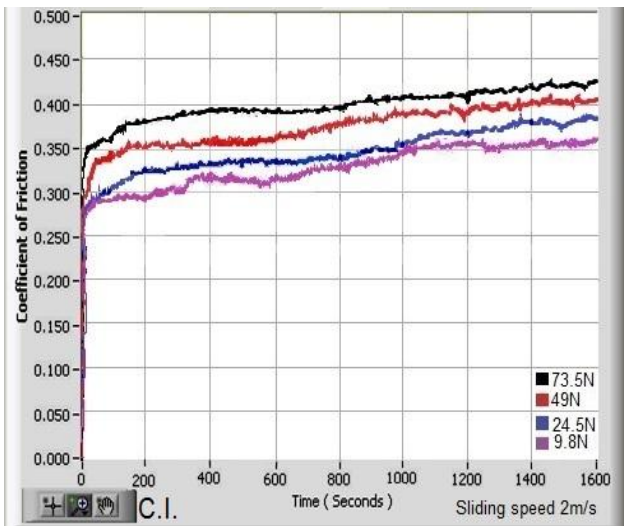
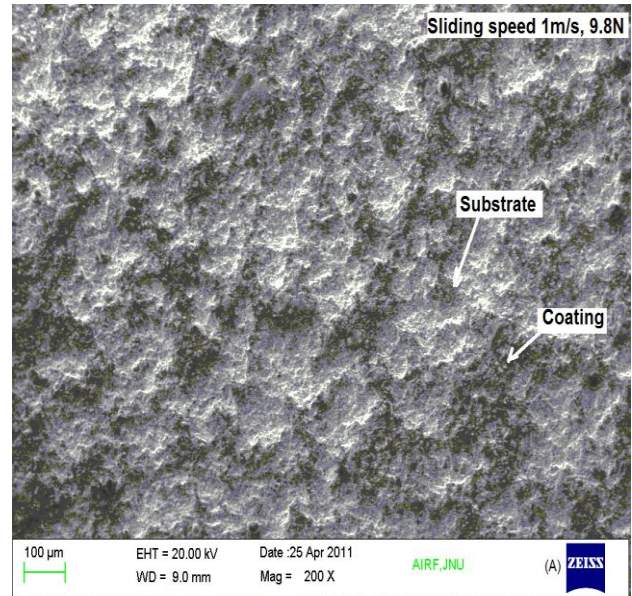


Fig. 15 COF C.I. at 1m/s

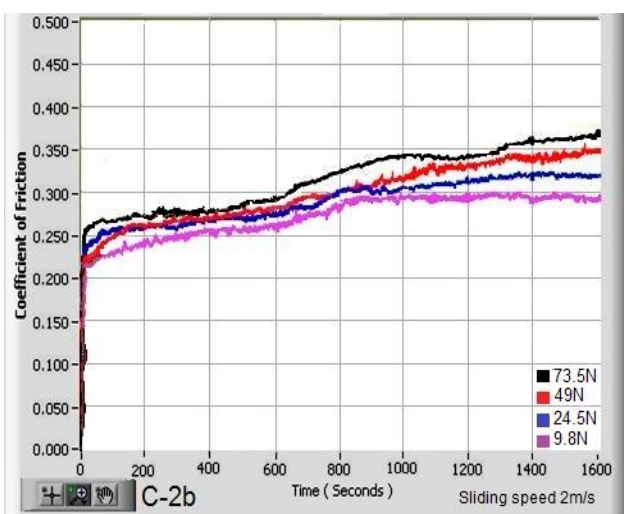
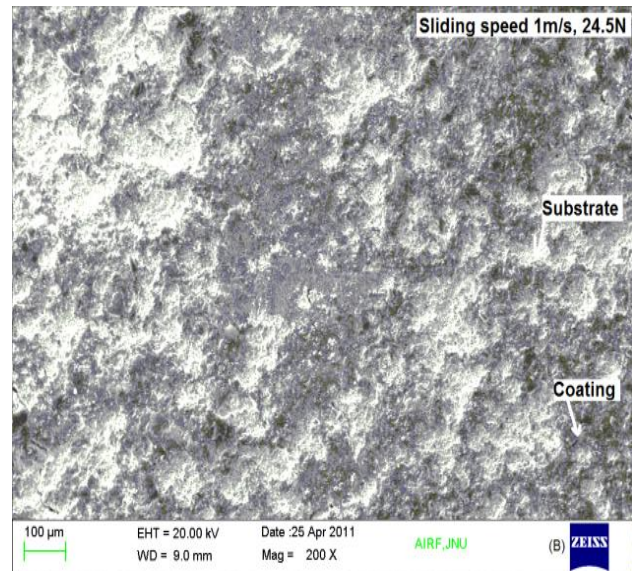
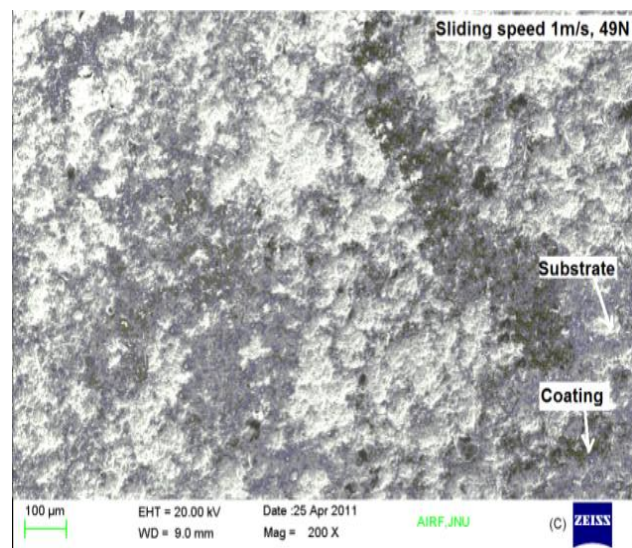
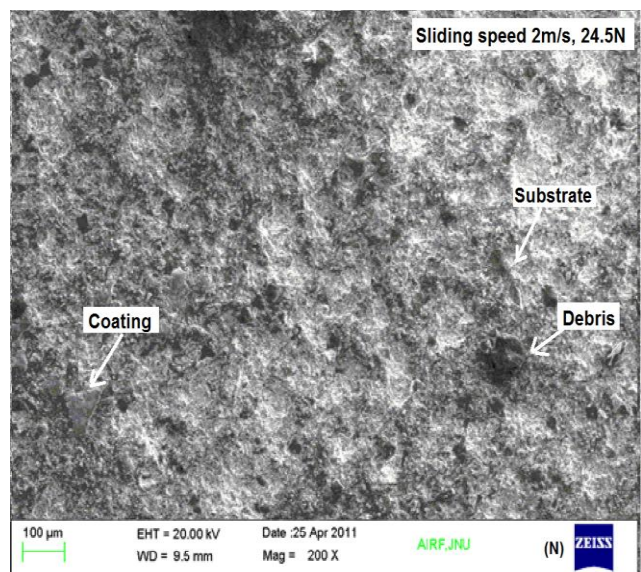
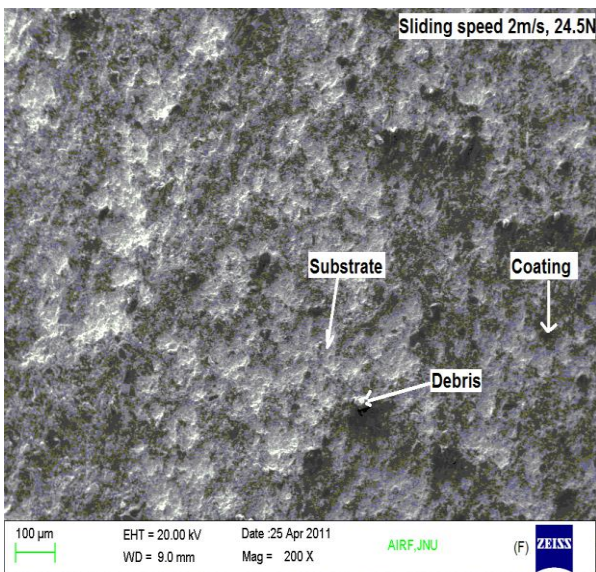
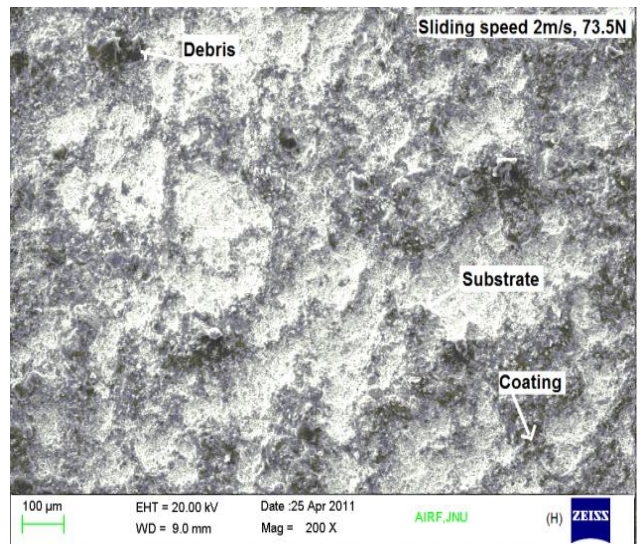
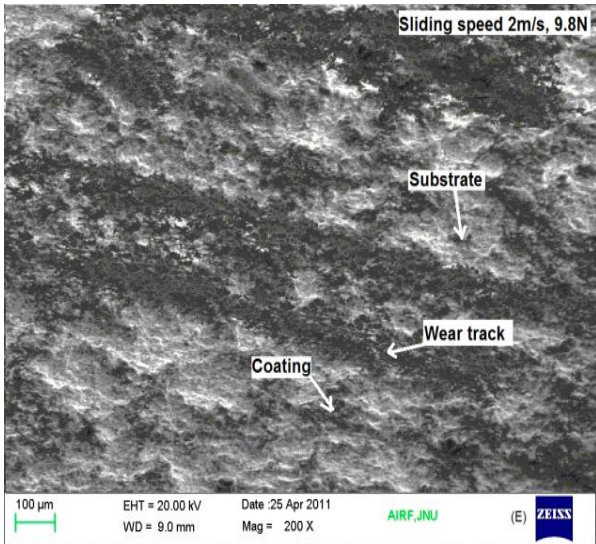
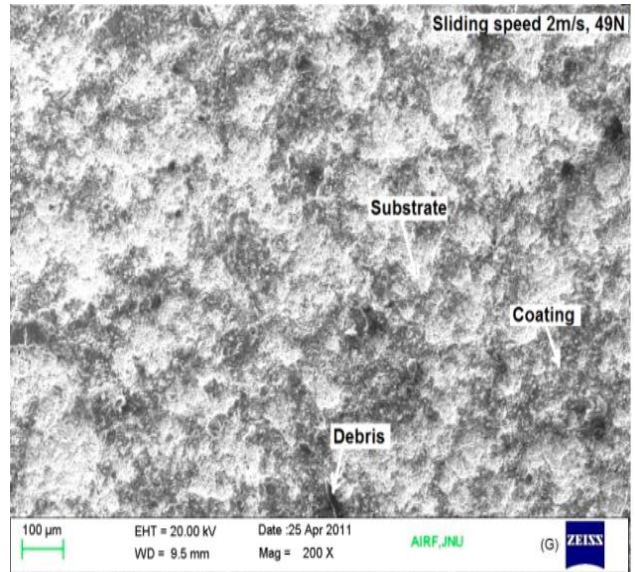
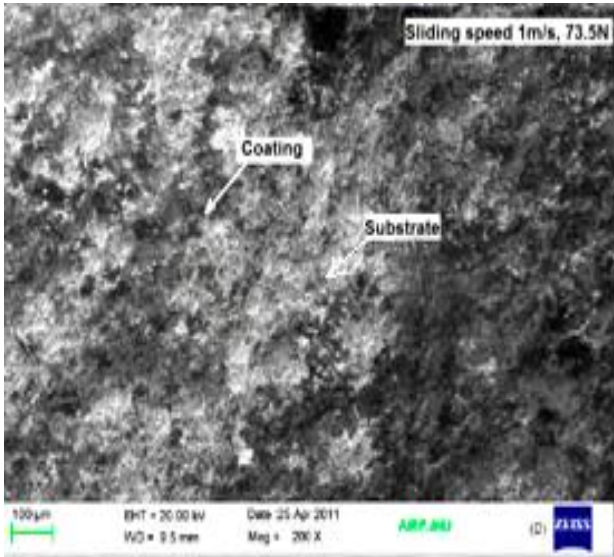


Fig. 16 COF C.I. at 2m/s





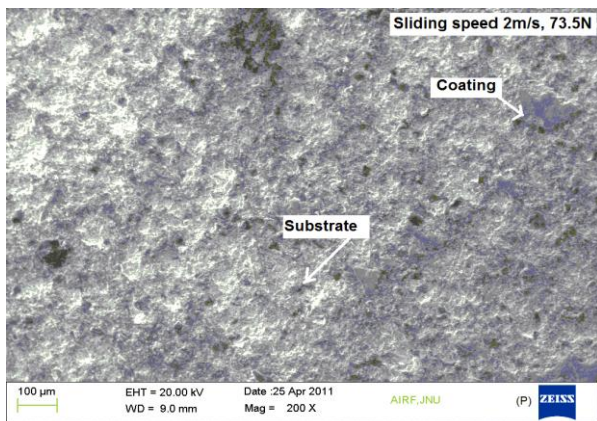
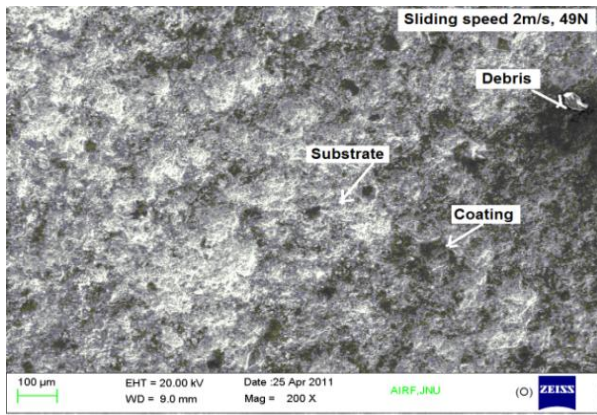


Fig. 17 Worn surfaces of the coatings

In this study the possibility of HVOF sprayed wear resistant ferrous coatings (K. Bobzin et al, 2008) have been tested which can actually be applied to engine cylinder bores. The wear behavior occurring under various loads and speeds has been studied. Wear values of the coating and the counterpart material have also been considered simultaneously to enhance the overall wear properties of the ferrous coatings. To further improve the ferrous coating the wear behavior occurring under various loads and speeds can also be studied.

## Conclusion

Two kinds of ferrous coated layers were deposited on A356 substrate, by HVOF spraying, and their microstructure and tribological properties were investigated with the following conclusions.

X-ray diffraction analysis showed the presence of elemental iron (Fe), FeNi,  $\alpha$ -Fe<sub>3</sub>O<sub>4</sub>,  $\alpha$ -Fe<sub>2</sub>O<sub>3</sub>, FeO,  $\alpha$ -FeCr, Cr<sub>2</sub>O<sub>3</sub> phases in coating C-1 and elemental iron (Fe),  $\alpha$ -Fe<sub>2</sub>O<sub>3</sub>,  $\gamma$ -Fe<sub>2</sub>O<sub>3</sub>, FeO, Fe<sub>3</sub>Ni,  $\alpha$ -FeCr phases in coating C-2.

Hardness of C-2 coating was higher than of C-1 coating and that had great influence on their tribological properties.

Tribological test (J. Rodr'iguez et al, 2003) results showed that for the investigated conditions both coatings had better wear properties than cast iron. Coating C-2 had even better wear properties than C-1 and the former could be adequate substitution for gray cast iron as a standard material for cylinder blocks.

## Acknowledgements

The authors wish to thank 'CAS' industry for supplying the powders used in this work and Mr. Udayveer (TERii), Mr. Rohit Batra (MMU) for the support offered during the investigation.

## References

- A. Edrisky a, T. Perry b, Y.T. Chengb, A.T. Alpas (2001), Wear of thermal spray deposited low carbon steelcoatings on aluminum alloys, *Wear* 25 ,pp1023–1033
- A. Edrisky a, T. Perry b, Y.T. Chengb, A.T. Alpas (2005), Wear Mechanism Maps for Thermal Spray Steel Coatings, *Metallurgical And Materials Transactions A*, pp2737-2750
- A. Edrisky a, T. Perry b, A.T. Alpas a, Investigation of scuffing damage in aluminum engines with thermal spray coatings, *Wear* 259 (2005), pp 1056–106
- A. Vencl, A. Rac, I. Bobić, Z. Mišković(2006) Tribological Properties of Al-Si Alloy A356 Reinforced With Al<sub>2</sub>O<sub>3</sub> Particles, *Tribology in industry*, Volume 28, No. 1&2, pp27-3
- Aleksandar Vencl, Mihailo Mrdak Ivana Cvijović (2006), Microstructures and tribological properties of ferrous coatings deposited by APS (Atmospheric Plasma Spraying) on Al-alloy substrate, *FME Transactions*, VOL. 34, No3, pp152-158
- Branagan, W.D. Swank, D.C. Haggard, J.R. Finckel Idaho, Wear resistant Amorphous and nano composit steel coatings, *National Engineering and Environmental Laboratory*, pp1-15
- Hieu Nguyen(2005), Manufacturing Processes and Engineering Materials Used in Automotive Engine Block, *Materials Science and Engineering Section B*, EGR250, pp 1-8
- J. Rodr'iguez, A. Mart'ın , R. Fernández , J.E. Fernández (2003), An experimental study of the wear performance of NiCrBSi thermal spray coatings, *Wear*, 255, pp950–955
- K. Bobzin, F. Ernst, J. Zwick, T. Schlaefer, D. Cook, K. Nassenstein, A. Schwenk, F. Schreiber, T. Wenz, G. Flores, and M. Hahn (2008), Coating Bores of Light Metal Engine Blocks with a Nanocomposite Material using the Plasma Transferred Wire Arc Thermal Spray Process, *Journal of Thermal Spray Technology*, Volume 17(3), pp344-351
- Mareike Hahn and Alfons Fischer (2010), Characterization of Thermal Spray Coatings for Cylinder Running Surfaces of Diesel Engines, *Journal of Thermal Spray Technology*, Volume 19(5), pp866-87
- Movahedi, M.H. Enayati, and C.C. Wong(2010), Structural and Thermal Behavior of Fe-Cr-Mo-P-B-C-Si Amorphous and Nanocrystalline HVOF Coatings, *Journal of Thermal Spray Technology*, Volume 19(5), pp1093-1099
- Narendra B. Dahotre, S. Nayak, and Oludele O. Popoola (2001), The Laser-Assisted Iron Oxide Coating of Cast Al Auto Engines, *JOM*, pp 45-46
- Nicholas J Breaux & Jerry K. Keska (2002), Application of a Pin-on-Disk Test to Determine Abrasive Wear, Proceedings of the 2002 ASEE Gulf-Southwest Annual Conference, *The University of Louisiana at Lafayette*, March, pp 20 – 22
- W. J. Kim1, J. G. Kim1, Y. S. Kim, Ismail Ozdemir, and Y. Tsunekawa(2007), Wear-Corrosion of Cast Iron Thermal Spray Coatings on Al Alloy for Automotive Components, *Metals and Materials International*, Vol. 13, No. 4, pp1-5